

## Suramin blocks nucleotide triphosphate binding to ribosomal protein L3 from *Trypanoplasma borreli*

Nuraly K. Avliyakov<sup>1,3</sup>, Julius Lukeš<sup>3</sup>, Andrey V. Kajava<sup>4</sup>, Bo Liedberg<sup>2</sup>, Ingemar Lundström<sup>2</sup> and Samuel P. S. Svensson<sup>1</sup>

<sup>1</sup>Department of Pharmacology, Faculty of Health Sciences; <sup>2</sup>Department of Applied Physics, University of Linköping, Sweden;

<sup>3</sup>Institute of Parasitology, Czech Academy of Sciences and Faculty of Biology, University of South Bohemia, České Budějovice, Czech Republic;

<sup>4</sup>Center for Molecular Modeling CIT, National Institutes of Health, Bethesda, MD, USA

Ribosomal protein L3 (L3) has been demonstrated to participate in formation of the peptidyltransferase center and is essential for its catalytic activity. In the present study we show that L3 is able to bind nucleotide triphosphates with high and specific affinity *in vitro*. L3 was serendipitously identified by screening of a genomic phage library from a primitive kinetoplastid flagellate *Trypanoplasma borreli* with the ATPase domain of the topoisomerase II gene as a probe. The cloned gene was overexpressed and purified as a his-tag fusion protein in *E. coli*. Radioligand binding experiments, using [ $\gamma$ -<sup>35</sup>S]ATP, showed that L3 is able to bind ATP but also GTP and UTP with similar high affinity (IC<sub>50</sub> 50–100 nM), while it has no ATPase activity. Furthermore, we showed that L3 has more than 500-fold higher affinity for nucleotide triphosphates compared to the corresponding nucleotide monophosphates and diphosphates. Molecular genetic and biochemical analyses allowed us to localize the NTP binding domain of L3 to the N-terminal 296 residues. Suramin, a polysulfonated naphthylamine derivative of urea, known for its chemotherapeutic effects completely inhibited the binding of [ $\gamma$ -<sup>35</sup>S]ATP at subclinical levels. Results obtained with surface plasmon resonance technology showed that suramin both forms weak multimolecular complexes with L3 and binds strongly to L3 in nearly stoichiometric amounts.

**Keywords:** nucleotide triphosphate; Kinetoplastida; ribosome; L3 protein; suramin.

*Trypanoplasma borreli* is a flagellate parasitizing the blood of freshwater fishes. Based on sequences of various conserved genes, it represents one of the earliest branches within the order Kinetoplastida [1–3], a group of primitive protozoans with many unique features [4]. By screening of a genomic phage library from *T. borreli*, using the ATPase domain of the topoisomerase II (topoII) gene as a probe, we identified a 1.4-kb DNA fragment containing the gene for ribosomal protein L3 (L3). L3 is vital for the function of the ribosome and has been shown to participate in or initiate the early steps of the ribosomal assembly [5], where it binds with high affinity to the 23S rRNA [6]. L3 is involved in the formation of the peptidyltransferase center and is essential for its catalytic activity [7–10]. The L3-binding site has been localized to a long double helix, containing a large internal loop and a sarcin/ricin loop in domain VI of 23S rRNA [11,12]. Additionally, L3 has been shown to possess extraribosomal functions, such as stimulation of helicase activity in *Escherichia coli* [13], or binding to yeast adenylyl cyclase-associated protein [14].

The method by which we have identified the L3, along with the results of the sequence database search which retrieved several ATP/GTPases, prompted us to further explore the

possibility of NTP binding by L3. This was indeed demonstrated in a series of experiments. *T. borreli* is a relative of highly pathogenic parasites of human *Trypanosoma brucei* and *T. cruzi*. *T. cruzi* is the causative agent of Chagas' disease which infects about 16–18 million people in Latin America [15], while *T. brucei* currently causes devastating epidemics of the African sleeping sickness in sub-Saharan Africa [16]. In the present study we demonstrate that the trypanocidal drug suramin has a high affinity to L3 and is able to inhibit the binding of [ $\gamma$ -<sup>35</sup>S]ATP at subclinical levels. Suramin is a polysulfonated naphthylamine derivative of urea that has been widely used since the 1920s for the treatment of human trypanosomiasis. The mechanism of action of suramin is not clear [17]. However, in cell-free preparations of *Crithidia fasciculata* suramin has been shown to inhibit protein synthesis [18]. Research on suramin has increased considerably since the discovery of its anti-AIDS and anti-cancer properties [17]. Our results may provide a new clue for the cytotoxic effects of this important drug.

### EXPERIMENTAL PROCEDURES

#### Organisms

*Trypanoplasma borreli* (strain Tt-Jh) and *Bodo saltans* (strain K1) isolated from the blood of tench (*Tinca tinca*), and the water of Lake Konstanz, respectively, were cultivated and their total DNA was isolated as described previously [2].

#### Cloning of ATPase domain of topoII gene of *B. saltans*

The ATPase domain of the topoII gene of *B. saltans* was amplified from the genomic DNA by PCR using two

Correspondence to S. P. S. Svensson, Department of Pharmacology, Faculty of Health Science, University of Linköping, SE-581 85 Linköping, Sweden. Fax: + 46 13 149106, Tel.: + 46 13 223456, E-mail: samsv@far.liu.se

**Abbreviations:** L3, ribosomal protein L3; topoII, topoisomerase II; SPR, surface plasmon resonance; GAP, GTPase-activating protein.

**Note:** the novel nucleotide sequence data published here have been deposited in the GenBank™ database under accession number AF225211. (Received 2 September 1999, revised 18 January 2000, accepted 20 January 2000)

degenerate primers P1 (5'-CATGTA/CCTC/GA/CTA/GC/AG/ACCG/AGAGAT/CGT AC-3') and P2 (5'-CCA/GTCT/GGCA/GTCCTGA/CTCT/GGTCATG/AA-3') based on conserved regions of the yeast and trypanosomatid topoII genes [20]. The amplified 1.5-kb fragment (30 cycles each consisting of 94 °C for 1 min, 54 °C for 1 min and 74 °C for 2 min and final extension 65 °C for 10 min) was cloned into the pT7Blue(R) vector (Novagen) and sequenced. The *NdeI*–*Bam*HI fragment was gel-purified, radiolabeled by nick translation, purified on a Sephadex G-50 column and used as a probe.

### Genomic library screening and cloning of L3 gene of *T. borreli*

A genomic library of *T. borreli* constructed in *E. coli* using partially *Sau*3AI-digested DNA and ligated into  $\lambda$ -GEM11 [3], obtained from P. A. M. Michels (Christian De Duve Institute of Cellular Pathology, Brussels, Belgium), was screened using the probe described above. Filters were prehybridized at 46 °C for 3 h, hybridized overnight at 46 °C, and washed twice with 3  $\times$  NaCl/Cit, 0.1% SDS for 5 min at room temperature, then once at 46 °C, 48 °C and 52 °C for 20 min each. Positive plaques were purified by two rounds of plating and hybridization, digested with *Eco*RI, resolved on a 1% agarose gel, blotted onto Hybond-N membrane (Amersham), and hybridized with the 1.5-kb ATPase domain of the topoII gene of *B. saltans* under conditions described above. The 1.4-kb hybridizing fragment was gel-isolated, cloned into *Eco*RI site of pBlue-script II SK<sup>-</sup> (Stratagene) and sequenced.

### Theoretical protein sequence analysis

The initial multiple sequence alignment was obtained by using the CLUSTALW program [20]. Manual corrections were made in some places of the alignment. Secondary structure was predicted using a PHD network server [21] and our multiple sequence alignment as a query. Alignment columns containing gaps were removed prior to the phylogenetic tree construction with GCG WISCONSIN program package (v 9.1) using the neighbor-joining algorithm [22].

### Overexpression and refolding of full-length L3

Two primers with inserted *Eco*RI and *Hind*III sites were used to amplify the full-length L3 gene by PCR using a *Pfu*I DNA polymerase (Stratagene). The amplified fragment was digested with *Eco*RI and *Hind*III, and inserted 'in frame' in the *Eco*RI and *Hind*III sites of the pET30a(+) expression vector (Novagen), creating pETL3, which was then overexpressed in *E. coli* cells BL21(DE3)pLysS after induction with IPTG and the His-L3 protein was purified on a His-Bind Resin column (Novagen) under denaturing conditions. Purified protein was analyzed by SDS/PAGE on 15% polyacrylamide gel using standard procedures [23]. Fractions containing the recombinant protein were combined and diluted to a protein concentration of 0.5 mg·mL<sup>-1</sup> in the refolding buffer A (40 mM Tris/HCl, pH 7.5, 300 mM NaCl, 0.1% (w/v) Nonidet P-40, 10% (w/v) glycerol, 10 mM 2-mercaptoethanol, 0.3 mM phenylmethylsulfonyl fluoride) containing 6.0 M urea. The recombinant protein was refolded by sequential dialysis against the refolding buffer A with decreasing concentrations of urea (4 M, 2 M, 0.5 M, and 0 M; each 8 h at 4 °C).

### Construction, overexpression and purification of truncated constructs

To generate 1–100L3 N-terminal truncated variant of L3, pETL3 was digested by *Kpn*I, resolved on a 1% agarose gel, purified and re-ligated, creating NTTL3. The long N-terminal fragment of L3 (1–296 N-terminal amino acids) was prepared by subcloning in frame the *Eco*RI–*Sa*I fragment from pETL3 into the same sites of pET30a(+) (LNTL3). The C-terminal fragment of L3 starting at Asp297 (297–416 C-terminal amino acids) was constructed by PCR amplification with primers containing the *Bam*HI and *Hind*III sites, and cloned into the same sites of pET30a(+) vector (CTL3). All constructs were confirmed by sequencing, overexpressed in *E. coli* BL21(DE3)-pLysS (except for the CTL3 construct), purified, and refolded as described above for pETL3. CTL3 was overexpressed in soluble form at 22 °C and purified on a His-Bind Resin column under native conditions. Purified CTL3 protein was dialyzed against the refolding buffer A in which Nonidet P-40 was replaced by 0.1% (w/v) Triton X-100.

### CD spectroscopy

CD spectra were generated using a CD6 spectrodichrograph (Jobin-Yvon, Longjumeau, France) in 0.05 and 0.1 cm quartz cells at 25 °C using protein concentrations of 0.5 or 0.25 mg·mL<sup>-1</sup> in 10 mM sodium phosphate buffer, pH 7.8. The samples were prepared immediately before the measurements by passing them through the NAP-10 column (Pharmacia) in 10 mM sodium phosphate buffer, pH 7.8. The CD spectra of L3 were measured in the same buffer in the absence or presence of 4 M urea. Protein concentration was determined according to [24].

### Radioligand binding of recombinant purified L3 protein

The [ $\gamma$ -<sup>35</sup>S]ATP-binding assays were performed as described previously [25] with the following modifications. In the samples, refolding buffer A was changed by gel filtration through the NAP-10 column into the buffer B (20 mM Tris/HCl, pH 7.5, 0.3 mM EDTA, 0.007% (v/v) Triton X-100, 7 mM dithiothreitol, 20% (w/v) glycerol). To remove any aggregates the samples were centrifuged at 12 000 *g* for 15 min before and after gel filtration. A standard reaction (100  $\mu$ L) in buffer B contained 2 nM [ $\gamma$ -<sup>35</sup>S]ATP (specific activity 1250 Ci·mmol<sup>-1</sup>) and 1–10  $\mu$ g of L3 with or without increasing concentrations of unlabeled competitive ATP, GTP, UTP, ADP, AMP and suramin. After incubation at room temperature for 20 min, the solution was filtered through a nitrocellulose membrane filter (Millipore HA 0.45  $\mu$ m) and presoaked in an ice-cold wash buffer (20 mM Tris/HCl, pH 7.5, 0.3 mM EDTA, 0.007% (v/v) Triton X-100, 1 mM dithiothreitol, 10% (w/v) glycerol). The filter was washed twice with 5 mL of ice-cold wash buffer and radioactivity retained in the filter was measured in a liquid scintillation counter. In saturation binding experiments, 1–10  $\mu$ g of L3 was incubated with increasing concentrations of [ $\gamma$ -<sup>35</sup>S]ATP (0.025–3 nM). Nonspecific binding was determined either in the absence of recombinant protein, or in the presence of 3  $\mu$ M GTP. The  $K_d$  for [ $\gamma$ -<sup>35</sup>S]ATP was determined by nonlinear regression of the saturation binding data with the following equation:  $Y = B_{\max} \times X / (K_d + X)$ , using GRAPHPAD PRISM (GraphPad Software, San Diego, CA, USA), where  $Y$  is the specific binding,  $X$  the concentration of radioligand,  $B_{\max}$  is the maximum binding and  $K_d$  the concentration of ligand required to reach the half-maximum binding. The radioligand

binding data from the competition experiments were fitted by nonlinear regression using GRAPHPAD PRISM to obtain  $IC_{50}$  values. Both  $K_d$  and  $IC_{50}$  values were derived from three independent experiments run in triplicate. The binding experiments with CTL3 were performed in buffer B containing 0.1% instead of 0.007% Triton X-100. pETL3 was digested with *Bgl*II and re-ligated, thus creating a plasmid with L3 insert out of the reading frame (pETcont). The protein expressed from this vector was used as a negative control in the binding experiments.

### Analysis of ATPase activity

ATPase assays were performed as described previously [26] with small modifications. Briefly, 2–4  $\mu$ g of purified L3 protein or 2.5  $\mu$ g of myosin (Sigma) were incubated at 37°C with trace amounts of  $[\gamma\text{-}^{32}\text{P}]\text{ATP}$  in total volume of 15  $\mu$ L containing 20 mM Tris/HCl, pH 7.5, 20 mM KCl, 1 mM dithiothreitol. After 15–20 min incubation reactions were stopped, and aliquots (2  $\mu$ L) were analyzed directly by TLC on polyethyleneimine-cellulose using 1 M formic acid and 0.5 M LiCl as solvents. The plates were dried and spots corresponding to inorganic phosphate ( $P_i$ ) and  $[\gamma\text{-}^{32}\text{P}]\text{ATP}$  were located by autoradiography.

### Surface plasmon resonance (SPR) measurements

Biospecific interactions were monitored by SPR using BIAcore X sensor technology (Pharmacia). The carboxylated dextran matrix on the sensor chip surface CM5 was first activated by 50 mM *N*-hydroxysuccinimide and 200 mM *N*-ethyl-*N'*-(dimethylaminopropyl)carbodiimide [27]. Then L3, diluted 1 : 10 (v/v) in the running buffer NaCl/Hepes (10 mM Na/Hepes, pH 7.4, 150 mM NaCl, 3.4 mM EDTA, 0.005% surfactant P20) was immobilized through amide coupling chemistry. Excess reactive sites were subsequently deactivated by injecting 1 M ethanolamine/HCl, pH 8.5. Binding experiments were performed by injecting increasing concentrations of suramin in NaCl/Hepes. Nonspecific binding was evaluated using the pETcont protein immobilized by the same procedures as L3, except that it was diluted in 10 mM sodium acetate, pH 4.8. The sensor chip was regenerated by a brief wash injection of 10 mM NaOH, 0.5 M NaCl. The flow was 5  $\mu\text{L}\cdot\text{min}^{-1}$  throughout the derivation and experimental procedure. Kinetic parameters were extracted from the sensorgrams using the BIA EVALUATION software (Pharmacia).

## RESULTS

### Identification and cloning of L3 of *T. borreli*

Using the 1.5-kb ATPase domain of *B. saltans* topoII as a probe to screen a genomic phage library of *T. borreli*, under low-stringency conditions, we were able to identify several hybridizing plaques, all of which contained a 1.4-kb *Eco*RI fragment, which was subcloned and sequenced. It contained a single open reading frame encoding a polypeptide of 416 amino acids, with predicted molecular mass of 47.63 kDa, and with 5' and 3' untranslated sequences 116 and 95 bp long, respectively. The presence of a single hybridizing band on Southern blots of total DNA cut with different restriction enzymes showed that L3 is a single-copy gene (data not shown).

Protein database search with the predicted polypeptide using BLAST program [28] revealed high homology with ribosomal proteins L3 from all extant groups of organisms. Although

*T. borreli* L3 has a high sequence identity with other L3 proteins, there are several differences specific to this sequence, reflected by its position on the basis of the eukaryotic tree (Fig. 1). The most closely related sequence (92% identity) was the L3 of *T. brucei*, from which only the 5' portion is available [29]. Generally, the eukaryotic L3 proteins are almost two times longer than their prokaryotic homologues. Throughout the alignment of L3 proteins, conserved regions alternate with less conserved ones (Fig. 2). This suggests that the difference between the eukaryotic and prokaryotic L3 proteins is the longer loop structure rather than additional domain(s). This also indicates that both prokaryotic and eukaryotic L3 proteins may have a similar core domain. The secondary structure prediction [21] based on multiple sequence alignment suggests that the core structure common to all L3 proteins consists of  $\beta$ -strands. The eukaryotic L3 proteins have additional long loops which may be  $\alpha$ -helical. Conformation of the refolded L3 protein was analyzed in the presence and absence of urea by CD spectroscopy. Far UV CD showed that L3 has  $\alpha$  and  $\beta$  conformations, which is in agreement with this prediction (data not shown). In an attempt to find sequence similarity with unrelated proteins, the generalized profile technique, a sensitive method for sequence database searches [30], was applied. The search showed that the transcription termination factor Rho from *Micrococcus luteus*, the ATP-dependent helicase from *Borrelia burgdorferi*, the putative DNA gyrase subunit (from *Streptomyces coelicolor* and the elongation factor  $1\alpha$  from *Cryptococcus neoformans* were the highest scoring unrelated sequences. However, the score was not high enough to decide whether this sequence similarity is significant or not. Another database search tool [31] identified a low sequence similarity between the N-terminal sequence (106–207) of L3 and Rabex-5 protein from *Bos taurus*, which displays GDP/GTP exchange activity on Rab5 protein [32].

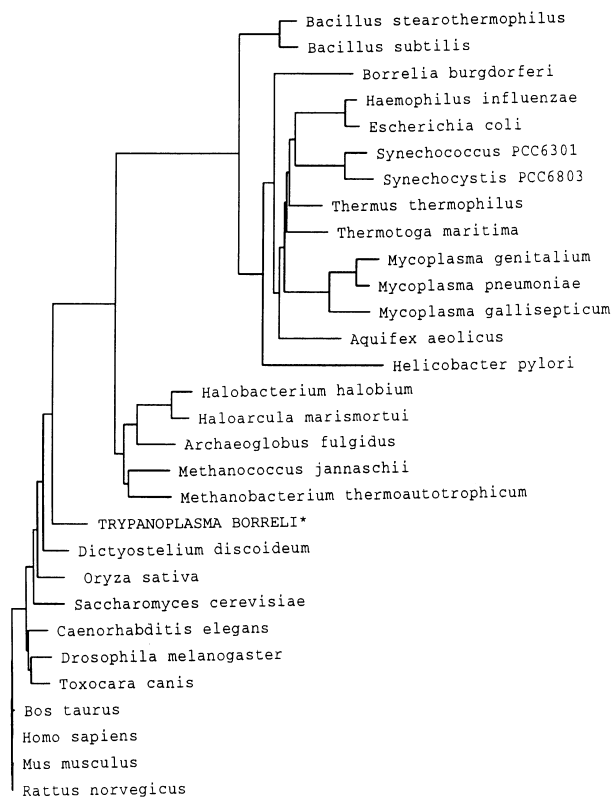


Fig. 1. Evolutionary analysis of the L3 protein sequences.

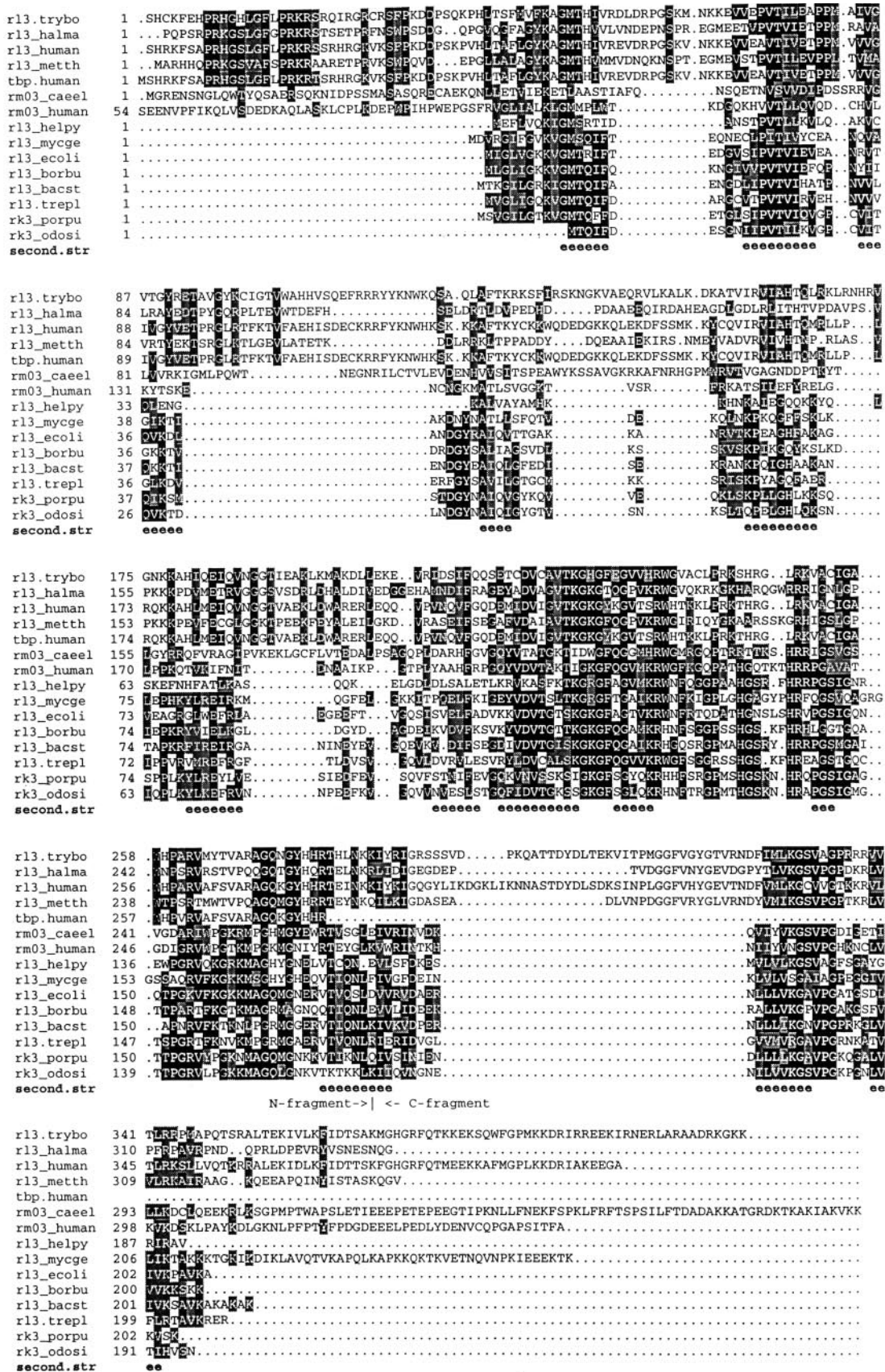
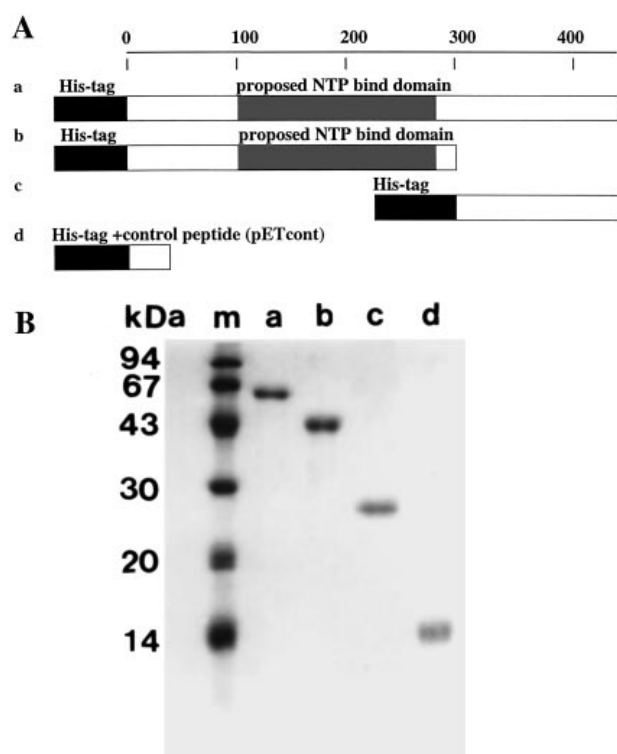


Fig. 2. Alignment of representative members of the ribosomal L3 protein family. Residues identical and conservatively substituted in at least 30% of the sequences are printed on black and gray background, respectively. The bottom line indicates the secondary structure prediction by PHD program [21] based on the multiple sequence alignment. Structure type is abbreviated: e, extended (sheet) conformation. Proteins which are not in the SWISSPROT database have the following abbreviations: r13.trybo, ribosomal L3 protein of *Trypanoplasma borreli*; tbp.human, human TAR binding protein, r13.trepl, ribosomal L3 protein of *Treponema pallidum*.



**Fig. 3. Truncated L3 proteins.** (A) Schematic representation of truncated L3 proteins overexpressed in *E. coli*, used in the filter-binding studies and analyzed by SPR: (a) full-length L3; (b) LNTL3; (c) CTL3; (d) pETcont. (B) Purification of full-length and truncated forms of L3 protein. The low molecular mass size markers (m), the equal amounts of purified full-length (a), and two truncated forms of L3 (b and c), and pETcont (d) proteins, were run in a 15% SDS/PAGE and stained with Coomassie Blue.

### Characterization of ATP-binding activity

To investigate the possible ATP-binding ability of L3, we cloned and overexpressed the full-length gene in the pET30a(+) vector. In spite of high level expression in the *E. coli* strain BL21(DE3)pLysS, all the recombinant overexpressed protein was localized in the inclusion bodies. Attempts to improve the efficiency of refolding of the recombinant protein, by using different growth temperatures in the range from 22 °C to 37 °C, and by decreasing the concentration of IPTG to 100  $\mu$ M were not successful. L3 was therefore purified from the inclusion bodies under denaturing conditions in the presence of 6 M urea (Fig. 3B). Affinity-purified protein was refolded by sequential dialysis against 4 M, 2 M, 0.5 M and 0 M urea in refolding buffer. Analysis by CD spectroscopy of the conformation of refolded protein in the presence or absence of urea clearly demonstrated that while in 4 M urea L3 was totally denatured, it regained its native structure during renaturation.

Figure 4A shows a [ $\gamma$ - $^{35}$ S]ATP-binding experiment with full-length recombinant L3 and increasing concentrations of ligand (with  $K_d = 1.3 \pm 0.2$  nM). To test the specificity of the [ $\gamma$ - $^{35}$ S]ATP binding, competition experiments with unlabeled ATP, GTP, UTP, ADP, AMP and the ATP-receptor antagonist suramin were performed. Increasing concentrations of these ligands were able to inhibit the binding of [ $\gamma$ - $^{35}$ S]ATP (Fig. 4B). Results showed that there was no significant difference between the different nucleotide triphosphates, however, the affinity for ADP and AMP was considerably

lower. The  $-\log IC_{50} \pm SEM$  values were  $7.2 \pm 0.1$  for ATP,  $7.4 \pm 0.2$  for GTP,  $7.0 \pm 0.2$  for UTP,  $5.8 \pm 0.3$  for ADP, and  $4.4$  for AMP. The binding of ATP was completely inhibited by micromolar concentrations of suramin,  $-\log IC_{50} = 7.2 \pm 0.1$  (Fig. 4B). The addition of increasing amounts of ATP (more than 10  $\mu$ M) into the binding buffer stimulated the aggregation

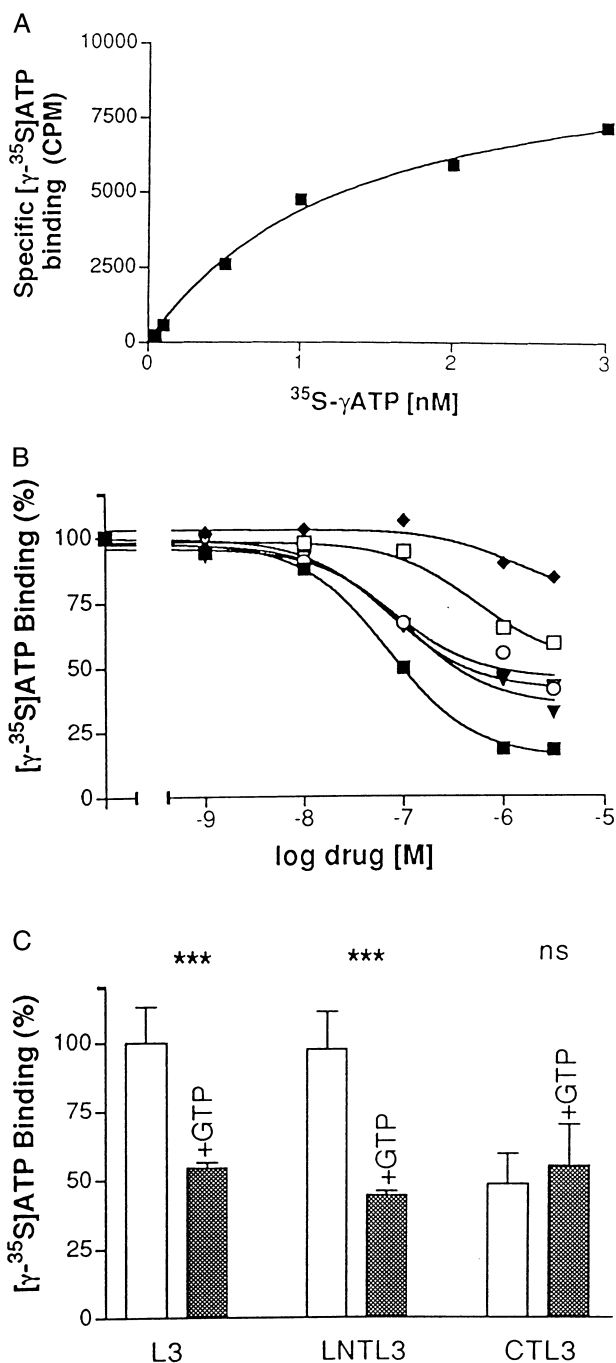


**Fig. 4. Radioligand binding studies of [ $\gamma$ - $^{35}$ S]ATP binding to purified L3.** (A) Representative saturation binding experiment with increasing concentrations of [ $\gamma$ - $^{35}$ S]ATP. Specific binding is defined as total binding minus nonspecific binding.  $K_d$  for [ $\gamma$ - $^{35}$ S]ATP was  $1.3 \pm 0.2$  nM,  $r^2$  0.96. (B) Competition binding studies of 2 nM [ $\gamma$ - $^{35}$ S]ATP by ATP (○), GTP (▽), UTP (▼), ADP (□), AMP (◆) and suramin (■) to L3. (C) Binding of [ $\gamma$ - $^{35}$ S]ATP, alone and in the presence of 3  $\mu$ M GTP to full-length and truncated forms of L3 including full-length L3, LNTL3 and CTL3 as shown in Fig. 3.



**Fig. 5. Analysis of possible ATPase activity.** Control sample without protein (1), myosin (2), and L3 protein (3) were incubated at 37°C with trace amounts of  $[\gamma\text{-}^{32}\text{P}]\text{ATP}$ . After 15–20 min incubation, products were separated by TLC using 1 M formic acid and 0.5 M LiCl as solvent, dried and visualized by autoradiography.

of L3, which was dependent on the protein concentration and salt conditions. This leads to an increased level of radioactivity retained in the filter membranes. Similar results were obtained using the ATP-agarose column. As we failed to elute L3 from the ATP-agarose column with a high concentration of competing unlabeled ATP, we concluded that L3 aggregated in the column (data not shown). Suramin, on the other hand, did not stimulate aggregation of L3 in any concentration tested. This explains why suramin was able to inhibit the  $[\gamma\text{-}^{35}\text{S}]\text{ATP}$  binding below the basal level (Fig. 4B). Furthermore, using myosin as a positive control, we have shown that L3 does not have ATPase activity (Fig. 5).

### Analysis of truncated constructs

A set of deletion mutants was constructed in order to localize the ATP-binding domain. As we anticipated that the N-terminal region could be responsible for this function, we have first removed 100 amino acids from the N-terminal part of L3 (NTTL3). The level of expression of this mutant construct was several times lower than that of the full-length L3, and was detected only in Western blot using the His-Tag antibodies,

suggesting that it is poorly expressed or degraded. However, the LNTL3 construct that encompasses the 296 N-terminal amino acids was readily overexpressed, purified and refolded (Fig. 3). Radioligand binding revealed that this construct binds  $[\gamma\text{-}^{35}\text{S}]\text{ATP}$  with affinity similar to the full-length L3, thus indicating that the ATP-binding domain is located within the N-terminal region (Fig. 4C).

To test whether the C-terminal fragment binds ATP, we prepared a construct that contains amino acids 297–416 (CTL3) (Fig. 3A). In contrast to LNTL3 and the full-length L3, about 40% of the CTL3 was overexpressed in the form of a soluble protein, which could therefore be purified under native conditions (Fig. 3B). As expected, CTL3 did not bind ATP (Fig. 4C).

### SPR measurements

To further characterize interactions with suramin, L3 was immobilized through amide coupling to the SPR sensor chip surface at a density of 7000 resonance units. Suramin was shown to bind to immobilized L3 with high and specific affinity. Nonspecific binding, defined as binding to pETcont, was always less than 10% of L3 binding (Fig. 6). The surface was completely regenerated by a brief wash with 10 mM NaOH/0.5 M NaCl. The binding behavior of suramin to L3 seems to be quite complex, as the association curve does not fit to a monophasic first order equation. The multiphase curve obtained could reflect heterogeneity of chemically immobilized L3 on the sensor chip, but the observed stoichiometry most likely reflects the association of several suramin molecules with each L3 molecule (Fig. 6). The data can be explained by the assumption that up to four suramin molecules associate with L3 of which, however, only one molecule shows strong binding to the protein (the remaining fraction binds also after 1000 s). The fast desorbing molecules are assumed to be associated with L3 through general electrostatic interactions. L3 bound to the dextran matrix corresponds to about 7000 Ru [1000 Ru (resonance units) is approximately  $1\text{ ng}\cdot\text{mm}^{-2}$  of molecules in the matrix]. The amount of associated/bound suramin just before rinsing corresponds to 600 Ru. As the molecular mass of L3 is 55.1 kDa and that of suramin about 1.4 kDa, we estimate that initially there are  $(600/1.4) \times (55/7000) \approx 3\text{--}4$  suramin molecules per L3 molecule. At the end of the discharge period the remaining signal is 100 Ru which corresponds to about 1 suramin per L3 molecule (Fig. 6). This slowly desorbing

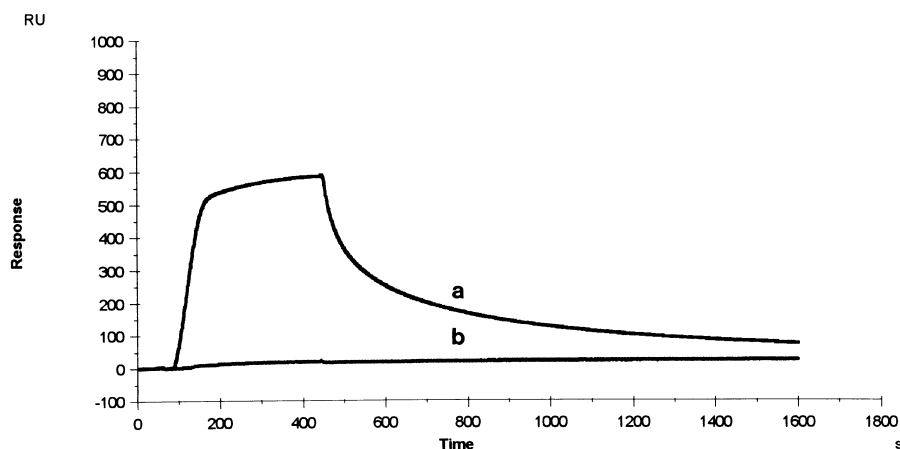


**Fig. 6. Real time binding of suramin analyzed by SPR.** L3 was immobilized to a carboxylated dextran matrix on a gold CM5 chip through amine coupling chemistry to which a  $1\ \mu\text{M}$  solution of suramin was injected (a). Nonspecific binding was evaluated using the pETcont protein as a control (b).

fraction has a kinetic dissociation constant of approximately  $1.6 \times 10^{-3} \text{ s}^{-1}$ .

## DISCUSSION

Attempts to amplify the ATPase domain of topoII gene of *T. borreli* using degenerate primers failed, whereas we were able to amplify its homologue in a related flagellate, *B. saltans*. As both species are members of the primitive suborder Bodonina [33], we used the topoII gene of *B. saltans* as a probe to screen the *T. borreli* phage library and Southern blots containing its digested DNA. Even at low-stringency conditions, the search was unsuccessful. However, we were able to identify several hybridizing plaques, all of which were identified as ribosomal protein L3.

The phylogenetic tree based on available full-size L3 sequences confirmed the early branching of *T. borreli*. The homology between the *T. brucei* and the *T. borreli* N-terminus is higher than the homology described for several conserved nuclear [1,3] and mitochondrial [2] genes of these flagellates. As the separation of these genera may have occurred more than 500 million years ago [2], such a conservation testifies to significant evolutionary constraints imposed on this region.

Based on the identification of L3 via the ATPase domain of topoII, and its limited sequence homology with ATP/GTPase binding proteins, we decided to investigate if L3 could bind NTP. Our results show that L3 is indeed able to bind ATP, and also GTP and UTP, with similar affinity (Fig. 4). Radioligand competition experiments with nucleotide mono-, di- and triphosphates showed that L3 has about 500-fold higher affinity to nucleotide triphosphates. Therefore we suggest that L3 is a NTP-binding protein with high specificity for the triphosphate moiety. Its long N-terminal domain is responsible for this binding, which does not seem to be based solely on electrostatic interactions as L3 has a very low affinity for NDP and NMP, and as the NTP-binding N-terminal domain contains less charged residues (pI 10.63) than the C-terminal domain (pI 11.03). Interestingly, mutations in yeast ribosomal L3, equivalent to the NTP-binding domain of *T. borreli*, affect the translational fidelity [34].

We suggest two possible biological functions of the NTP-binding by L3 protein in the ribosome. It has been reported that ribosomes from both the lower and higher eukaryotes possess tightly associated ATP/GTPase and ATPase activities [35–37]. The intrinsic ATPase activity of ribosomes facilitates the release of the deacylated tRNA from the E-site [37]. So far, ribosomal components involved in the NTPase activity remain unknown. Although it has yet to be demonstrated *in vivo*, we suggest that L3 might be responsible, perhaps in cooperation with other proteins, for NTP binding in the ribosome. Participation of L3 protein in the formation of a peptidyltransferase center [7–10] is consistent with this conclusion.

L3 protein binds to the highly conserved sarcin/ricin loop of the 23S rRNA [12] which is situated near the GTPase domain [12,16,38]. It is also the receptor site for the pokeweed antiviral protein [39]. This loop is crucial for ribosome function, as it constitutes one of the binding sites for the elongation factors [40–42] to which L3 has been cross-linked [43]. The C-terminal domain of L7/12 protein might be the GTPase-activating protein (GAP) in the ribosome [44]. However, it does not itself have the GAP activity *in vitro* [45]. So far, the GAP components within the 50S and 60S ribosomal subunits remain to be identified. Due to its NTP-binding activity, L3 becomes a likely member, along with the highly conserved sarcin/ricin

loop and ribosomal proteins L7/12, L10 and L11 [46,47], of this GAP structure.

Interestingly, the NTP-binding function of L3 can be completely inhibited by suramin which binds, as confirmed by SPR in real time, to L3 at very low concentrations. Suramin is one of the first widely accepted anti-parasitic drugs and it has been used world-wide against trypanosomes for over 70 years. The interest in suramin research has increased considerably as the drug was also found to have anti-cancer and anti-AIDS properties [17]. The sequence similarity between human and trypanosome L3 genes may explain cytotoxicity, which is the major disadvantage of this drug. The binding activity of suramin seems in most cases to be of electrostatic nature [17]. For example, its binding to phosphoglycerate kinase has been mapped to two clusters of positively charged amino acids on the surface of the enzyme [48]. Recent data have shown that suramin is able to bind and inhibit protein-tyrosine phosphatases. This binding is also likely to be electrostatic, as the affinity of suramin was reduced by mutating arginine to alanine within the active site of the phosphates [49]. Indeed, especially in its putative NTP-binding domain, *T. borreli* L3 is a highly positively charged protein. The positive charge may also be the cause for the large number of suramin molecules weakly associated with L3 as revealed by the SPR study.

Previous results have shown that suramin affects both the ribosome function *in vivo* and protein synthesis *in vitro*. In *Trypanosoma rhodesiense*, suramin induced lesions to the ribosome, suggesting that the ribosomal protein synthesis machinery is inactivated [50]; and in cell-free preparations of *C. fasciculata*, suramin inhibited protein synthesis [18]. Our results show that suramin binds to L3 and inhibits ATP-binding at subclinical levels, thus suggesting that L3 might be a new and important target for the widely used drug.

## ACKNOWLEDGMENTS

We thank Dr P. A. M. Michels (Christian De Duve Institute of Cellular Pathology, Brussels, Belgium) for kindly providing the *T. borreli* genomic library, and Dr Dick Andersson for help with CD spectroscopy. This research was supported by grants of the Swedish Natural Science Research Council, Swedish Medical Research Council (K1999-14P-013050-01A, K1999-14X-013046-01A) and the Grant Agency of the Czech Academy of Sciences A6022903. N. K. A. has also been supported by a short-term Swedish Institute scholarship.

## REFERENCES

- Maslov, D.A., Avila, H.A., Lake, J.A. & Simpson, L. (1994) Evolution of RNA editing in kinetoplastid protozoa. *Nature* **368**, 345–348.
- Lukeš, J., Arts, G.J., van den Burg, J., de Haan, A., Opperdoes, F., Sloof, P. & Benne, R. (1994) Novel pattern of editing regions in mitochondrial transcripts of the cryptobiid *Trypanoplasma borreli*. *EMBO J.* **13**, 5086–5098.
- Wiemer, E.A., Hannaert, V., van den IJssel, P.R., Van Roy, J., Opperdoes, F.R. & Michels, P.A. (1995) Molecular analysis of glyceraldehyde-3-phosphate dehydrogenase in *Trypanoplasma borelli*: an evolutionary scenario of subcellular compartmentation in kinetoplastida. *J. Mol. Evol.* **40**, 443–454.
- Donelson, J.E., Gardner, M.J. & El-Sayed, N.H. (1999) More surprises from Kinetoplastida. *Proc. Natl Acad. Sci. USA* **96**, 2579–2581.
- Nowotny, V. & Nierhaus, K.H. (1982) Initiator proteins for the assembly of the 50S subunit from *Escherichia coli* ribosomes. *Proc. Natl Acad. Sci. USA* **79**, 7238–7242.
- Speirer, P. & Zimmermann, R.A. (1976) RNA–protein interactions in

- the ribosome. Binding of proteins L1, L3, L6, L13 and L23 to specific fragments of the 23S RNA. *FEBS Lett.* **68**, 71–75.
7. Hampl, H., Schulze, H. & Nierhaus, K.H. (1981) Ribosomal components from *Escherichia coli* 50S subunits involved in the reconstitution of peptidyltransferase activity. *J. Biol. Chem.* **256**, 2284–2288.
  8. Franceschi, F.J. & Nierhaus, K.H. (1990) Ribosomal proteins L15 and L16 are mere late assembly proteins of the large ribosomal subunit. Analysis of an *Escherichia coli* mutant lacking L15. *J. Biol. Chem.* **265**, 16676–16682.
  9. Green, R. & Noller, H.F. (1997) Ribosomes and translation. *Annu. Rev. Biochem.* **66**, 679–716.
  10. Khaitovich, P., Mankin, A.S., Green, R., Lancaster, L. & Noller, H.F. (1999) Characterization of functionally active subribosomal particles from *Thermus aquaticus*. *Proc. Natl Acad. Sci. USA* **96**, 85–90.
  11. Leffers, H., Egebjerg, J., Andersen, A., Christensen, T. & Garrett, R.A. (1988) Domain VI of *Escherichia coli* 23S ribosomal RNA. Structure, assembly and function. *J. Mol. Biol.* **204**, 507–522.
  12. Uchiumi, T., Sato, N., Wada, A. & Hachimori, A. (1999) Interaction of the sarcin/ricin domain of 23S ribosomal RNA with proteins L3 and L6. *J. Biol. Chem.* **274**, 681–686.
  13. Soultanas, P., Dillingham, M.S. & Wigley, D.B. (1998) *Escherichia coli* ribosomal protein L3 stimulates the helicase activity of the *Bacillus stearothermophilus* PcrA helicase. *Nucleic Acids Res.* **26**, 2374–2379.
  14. Yanagihara, C., Shinkai, M., Kariya, K., Yamawaki-Kataoka, Y., Hu, C.D., Masuda, T. & Kataoka, T. (1997) Association of elongation factor 1 alpha and ribosomal protein L3 with the proline-rich region of yeast adenylyl cyclase-associated protein CAP. *Biochem. Biophys. Res. Commun.* **232**, 503–507.
  15. WHO (1991) *Control of Chagas' Disease, WHO Technical Series #811*. World Health Organization, Geneva.
  16. Smith, D.H., Pepin, J. & Stich, A.H. (1998) Human African trypanosomiasis: an emerging public health crisis. *Br. Med. Bull.* **54**, 341–355.
  17. Voogd, T.E., Vansterkenburg, E.L., Wilting, J. & Janssen, L.H. (1993) Recent research on the biological activity of suramin. *Pharmacol. Rev.* **45**, 177–203.
  18. Kahan, D., Zahalsky, A.C. & Hutner, S.H. (1968) Protein synthesis in cell-free preparations of *Crithidia fasciculata*. *J. Protozool.* **15**, 385–390.
  19. Strauss, P.R. & Wang, J.C. (1990) The TOP2 gene of *Trypanosoma brucei*: a single-copy gene that shares extensive homology with other TOP2 genes encoding eukaryotic DNA topoisomerase II. *Mol. Biochem. Parasitol.* **38**, 141–150.
  20. Higgins, D.G., Thompson, J.D. & Gibson, T.J. (1996) Using CLUSTAL for multiple sequence alignments. *Methods Enzymol.* **266**, 383–402.
  21. Rost, B., Sander, C. & Schneider, R. (1994) PHD – an automatic mail server for protein secondary structure prediction. *Comput. Appl. Biosci.* **10**, 53–60.
  22. Kimura, M. (1983) *The Neural Theory of Evolution*. Cambridge University Press, Cambridge.
  23. Laemmli, U.K. (1970) Cleavage of structural proteins during the assembly of the head of bacteriophage T4. *Nature* **227**, 680–685.
  24. Bradford, M.M. (1976) A rapid and sensitive method for the quantitation of microgram quantities of protein utilizing the principle of protein-dye binding. *Anal. Biochem.* **72**, 248–254.
  25. Sekimizu, K., Bramhill, D. & Kornberg, A. (1987) ATP activates dnaA protein in initiating replication of plasmids bearing the origin of the *E. coli* chromosome. *Cell* **50**, 259–265.
  26. Kornberg, A., Scott, J.F. & Bertsch, L.L. (1978) ATP utilization by rep protein in the catalytic separation of DNA strands at a replicating fork. *J. Biol. Chem.* **253**, 3298–3304.
  27. Liedberg, B. & Johansen, K. (1998) Affinity biosensing based on surface plasmon detection. In *Methods in Biotechnology* (Rogers, K.R. & Mulchandani, A., eds), Vol. 7, pp. 31–53. Humana Press, Totowa, NJ.
  28. Altschul, S.F., Madden, T.L., Schaffer, A.A., Zhang, J., Zhang, Z., Miller, W. & Lipman, D.J. (1997) Gapped BLAST and PSI-BLAST: a new generation of protein database search programs. *Nucleic Acids Res.* **25**, 3389–3402.
  29. Djikeng, A., Agufa, C., Donelson, J.E. & Majiwa, P.A. (1998) Generation of expressed sequence tags as physical landmarks in the genome of *Trypanosoma brucei*. *Gene* **221**, 93–106.
  30. Bucher, P., Karplus, K., Moeri, N. & Hofmann, K. (1996) A flexible motif search technique based on generalized profiles. *Comput. Chem.* **20**, 3–23.
  31. Worley, K.C., Wiese, B.A. & Smith, R.F. (1995) BEAUTY: an enhanced BLAST-based search tool that integrates multiple biological information resources into sequence similarity search results. *Genome Res.* **5**, 173–184.
  32. Horiuchi, H., Lippe, R., McBride, H.M., Rubino, W., Woodman, P., Stemmark, H., Rybin, V., Wilm, M., Ashman, K., Mann, M. & Zeña, M. (1997) A novel Rab5 GDP/GTP exchange factor complexed to Rabaptin-5 links nucleotide exchange to effector recruitment and function. *Cell* **90**, 1149–1159.
  33. Blom, D., de Haan, A., van den Berg, M., Sloof, P., Jirků, M., Lukeš, J. & Benne, R. (1998) RNA editing in the free-living bodonid *Bodo saltans*. *Nucleic Acids Res.* **26**, 1205–1213.
  34. Peltz, W.S., Hammell, A.B., Cui, Y., Yasenchak, J., Puljanowski, L. & Dinman, J.D. (1999) Ribosomal protein L3 mutants alter translational fidelity and promote rapid loss of the yeast killer virus. *Mol. Cell Biol.* **19**, 384–392.
  35. Grummt, F., Grummt, I. & Erdmann, V.A. (1974) ATPase and GTPase activities isolated from rat liver ribosomes. *Eur. J. Biochem.* **43**, 343–348.
  36. Miyazaki, M. & Kagiyama, M. (1990) Soluble factor requirements for the *Tetrahymena* peptide elongation system and the ribosomal ATPase as a counterpart of yeast elongation factor 3 (EF-3). *J. Biochem. (Tokyo)* **108**, 1001–1008.
  37. El'skaya, A.V., Ovcharenko, G.V., Palchevskii, S.S., Petrushenko, Z.M., Triana-Alonso, F.J. & Nierhaus, K.H. (1997) Three tRNA binding sites in rabbit liver ribosomes and role of the intrinsic ATPase in 80S ribosomes from higher eukaryotes. *Biochemistry* **36**, 10492–10497.
  38. Ryan, P.C., Lu, M. & Draper, D.E. (1991) Recognition of the highly conserved GTPase center of 23S ribosomal RNA by ribosomal protein L11 and the antibiotic thiostrepton. *J. Mol. Biol.* **20**, 1257–1268.
  39. Hudak, K.A., Dinman, J.D. & Tumer, N.E. (1999) Pokeweed antiviral protein accesses ribosomes by binding to L3. *J. Biol. Chem.* **274**, 3859–3864.
  40. Munishkin, A. & Wool, I.G. (1997) The ribosome-in-pieces: binding of elongation factor EF-G to oligoribonucleotides that mimic the sarcin/ricin and thiostrepton domains of 23S ribosomal RNA. *Proc. Natl Acad. Sci. USA* **94**, 12280–12284.
  41. Moazed, D., Robertson, J.M. & Noller, H.F. (1988) Interaction of elongation factors EF-G and EF-Tu with a conserved loop in 23S RNA. *Nature* **334**, 362–364.
  42. Hausner, T.P., Atmadja, J. & Nierhaus, K.H. (1987) Evidence that the G2661 region of 23S rRNA is located at the ribosomal binding sites of both elongation factors. *Biochimie* **69**, 911–923.
  43. Maassen, J.A. & Moller, W. (1981) Photochemical cross-linking of elongation factor G to 70S ribosomes from *Escherichia coli* by 4-(6-formyl-3-azidophenoxy) butyrimidate. *Eur. J. Biochem.* **115**, 279–285.
  44. Moller, W., Schrier, P.I., Maassen, J.A., Zantema, A., Schop, E., Reinalda, H., Cremers, A.F. & Mellema, J.E. (1983) Ribosomal proteins L7/L12 of *Escherichia coli*. Localization and possible molecular mechanism in translation. *J. Mol. Biol.* **163**, 553–573.
  45. Donner, D., Villems, R., Liljas, A. & Kurland, C.G. (1978) Guanosinetriphosphatase activity dependent on elongation factor Tu and ribosomal protein L7/L12. *Proc. Natl Acad. Sci. USA* **75**, 3192–3195.
  46. Schmidt, F.J., Thompson, J., Lee, K., Dijk, J. & Cundliffe, E. (1981) The binding site for ribosomal protein L11 within 23S

- ribosomal RNA of *Escherichia coli*. *J. Biol. Chem.* **256**, 12301–12305.
47. Beauclerk, A.A., Cundliffe, E. & Dijk, J. (1984) The binding site for ribosomal protein complex L8 within 23S ribosomal RNA of *Escherichia coli*. *J. Biol. Chem.* **259**, 6559–6563.
48. Hart, D., Langridge, A., Barlow, D. & Sutton, B. (1989) Antiparasitic drug design. *Parasitol. Today* **5**, 117–120.
49. Zhang, Y.L., Keng, Y.F., Zhao, Y., Wu, L. & Zhang, Z.Y. (1998) Suramin is an active site-directed, reversible, and tight-binding inhibitor of protein-tyrosine phosphatases. *J. Biol. Chem.* **273**, 12281–12287.
50. Macadam, R.F. & Williamson, J. (1974) Drug effects on the fine structure of *Trypanosoma rhodesiense*: suramin, tryparsamide and mapharside. *Ann. Trop. Med. Parasitol.* **68**, 301–306.